A spatial particle correlation-function analysis in non-isothermal dilute particle-laden turbulent flows

Enrica Masi, Pascal Fede, Olivier Simonin

A spatial particle correlation-function analysis in non-isothermal dilute particle-laden turbulent flows

Enrica Masi*, Pascal Fede and Olivier Simonin
Institut de Mécanique des Fluides de Toulouse (IMFT), Université de Toulouse, CNRS, INPT, UPS, Toulouse, FRANCE

Abstract

In dilute gas-solid turbulent flows, as that encountered, for example, in pulverized coal combustion processes, the correct prediction of the non-isothermal/reactive particle-laden turbulent mixture relies on the accuracy of the modeling of the local and unsteady particle behavior, which affects the hydro-thermodynamic coupling and the heat transfer and transport in and between the phases and at wall. In very dilute mixtures composed of highly inertial solid particles, such a local and unsteady behavior is the result of the particle interactions with very distant and independent turbulent eddies, namely with different dynamic and thermal turbulent scales. Such interactions strongly modify the local particle velocity and temperature distributions, changing the local evolution of the properties of the dispersed phase. Their knowledge is thus crucial when modeling unsteady particle-laden turbulent flows. In this work, the focus is on the particle temperature distribution. Its characterization is provided by means of an analysis of the two-particle correlation functions in the frame of the direct numerical simulation of non-isothermal homogeneous isotropic, statistically stationary, turbulent flows.

Keywords: Particle-laden turbulent flows, non-isothermal flows, very dilute regime

1. Introduction

Modeling non-isothermal/reactive particle-laden turbulent flows, requires a deep understanding of the dispersed phase both from a dynamic and a thermal point of view. In particular, when the dispersed phase is modeled as a continuum in the frame of the PDF moment approach, the understanding of the local particle behavior is crucial in order to characterize with high fidelity particle statistical properties. From an Eulerian point of view, the characterization of the particle velocity and temperature distributions is very important for the modeling of the local and instantaneous (i.e., DNS or LES) particle-laden flows. In the literature, several unsteady Eulerian approaches exist, able to predict the particulate phase in a local fashion. For very low Stokes numbers, the particle velocity and temperature distributions may be modeled by the unique first-order moment [12] (i.e., the ensemble average of particle velocities and temperatures) since each particle responds rapidly to the local changes of the fluid keeping strong correlations with the surrounding flows and with the neighboring particles as well. For very low Stokes numbers, methods based on a Taylor expansion of the particle velocity and temperature equations may also be used [6, 7]. For Stokes numbers greater than unity (based on the Kolmogorov time scale) the monovalue assumption generally fails since particle velocity and temperature exhibit a local distribution which is characterized by high order central moments. The larger is the particle inertia, the more important is their contribution. In this case, in order to be effective, moment approaches required to account for high order moments as well [20, 8, 9, 24, 16, 23, 3]. The understanding of the particle velocity and temperature distributions is therefore an important point of the particle Eulerian modeling in turbulent flows.

In order to gain insight in the understanding of the local particle behavior, Février, Simonin & Squires [8] developed a formalism able to explain the nature of velocity correlations between neighboring particles. The authors suggest a point of view about the question, why heavy particles are less spatially correlated than light particles at short rather than long separation distances? This concern was investigated using spatial velocity correlations computed between any two separate particles. At the scalar limit, such a two-point correlation function approaches that of the fluid, behaving exponentially as modeled in one-phase flow by Hinze [10] and converging to the particle kinetic energy for distances tending to zero. An increase in particle inertia leads to lose part of the correlation in motion for neighboring particles with a consequent decrease in correlation at the zero-distance limit. This phenomenon was explained by analogy to the kinetic theory of dilute gases [1]: at the limit of very large inertia, particles move chaotically behaving like molecules in a dilute gas. In intermediary regimes, particles partially adapt to the turbulence because of their response times, magnifying any microscopic difference coming from their initial conditions: this behavior leads to trajectories crossing and particles may find themselves nearby when coming from interactions with distant and independent turbulent eddies. The formalism proposed by Février et al. [8] allows to take into account the effects of the inertia on the particle motion by partitioning the velocity in two contributions: first, the mesoscopic Eulerian particle velocity field, which is a continuous field shared by all the particles and accounting for correlations between particles and between particles and the fluid; second, a random spatially-uncorrelated contribution associated with each particle and satisfying the molecular-chaos assumption. It is referred to as uncorrelated velocity and characterized in terms of Eulerian fields of particle velocity moments. The mesoscopic Eulerian formalism is found to be very useful for the understanding of particle-particle and fluid-particle interaction mechanisms [11]. It has been used to investigate the spatial characteristics of the particle velocity field in a turbulent channel flow with and without inter-particle collisions [22] and it was compared with a two-point probability density function method finding strong connections when modeling spatial characteristics of inertial particles [21]. Such an approach, providing local and instantaneous Eulerian fields for the dispersed phase, has been used to derive the Eulerian approach for particle-laden turbulent flows in a LES framework [18, 14]. In the spectrum of the Eulerian approaches it is found particularly adequate to predict inertial particle-laden turbulent flows in the presence of unsteady phenomena or in complex geometries [19] and its use in non-isothermal conditions remains a timely topic of research. The goal of this study is to

* corresponding author: emasi@imft.fr

improve the understanding of the particle temperature distribution and of the mechanisms of heat transfer and transport in order to improve the Eulerian modeling, confirming the validity of a recent extension of the formalism to non-isothermal conditions [15, 17]. Applications in reactive two-phase flows motivate this study.

2. Two-point particle correlation functions

In order to characterize the particle temperature distribution, particle-particle (also referred to as two-point particle) correlation functions are investigated. Two-point correlation functions are computed using three different methods. They are here briefly explained and formalized in the frame of homogeneous, isotropic, and statistically stationary conditions, where particle properties (velocity or temperature) only get a fluctuating nature around a zero mean. The first method accounts for the product between the temperatures of any pair of particles m and n (with $m \neq n$) separated by a distance r. The spatial correlation function may then be written as:

$$R_\theta^{pp}(r) = \overline{\{T_p^{(m)}(t)T_p^{(n)}(t)\big| \quad |\boldsymbol{x}_p^{(m)}(t) - \boldsymbol{x}_p^{(n)}(t)| = r\}} \tag{1}$$

where curly brackets and over line denote instantaneous average over all the particle pairs and temporal average, respectively. An alternative (cheaper) method, employing instantaneous particle Eulerian fields, was proposed by Février et. [8]. In order to obtain instantaneous particle Eulerian fields, Kaufmann et al. [11] proposed a projection procedure which uses a well defined projection filter. The projection procedure may be written as follows:

$$\tilde{n}_p(\boldsymbol{x},t) = \sum_m w(\boldsymbol{x}_p^{(m)}(t) - \boldsymbol{x}) \tag{2}$$

$$\tilde{n}_p(\boldsymbol{x},t)\widetilde{T}_p(\boldsymbol{x},t) = \sum_m w(\boldsymbol{x}_p^{(m)}(t) - \boldsymbol{x})T_p^{(m)}(t) \tag{3}$$

where $\tilde{n}_p(\boldsymbol{x},t)$ and $\widetilde{T}_p(\boldsymbol{x},t)$ are approximation of local and instantaneous (i.e. mesoscopic) particle number density and temperature fields, respectively, expected to be exact when the number of particle realizations conditional on a given fluid flows $\mathcal{N}_p \to \infty$. The quantity w represents a projection filter. Février et al. [8] used a technique which may be considered as equivalent to employ the projection procedure using a box filter:

$$w(\boldsymbol{x}_p^{(m)} - \boldsymbol{x}) = \begin{cases} \dfrac{1}{\Delta x^3}, & \text{if} \quad |\boldsymbol{x}_{p,i}^{(m)} - \boldsymbol{x}_i| \leq \Delta x/2 \\ 0, & \text{otherwise} \end{cases} \tag{4}$$

Kaufmann et al. [11] proposed a Gaussian filter which reads:

$$w(\boldsymbol{x}_p^{(m)} - \boldsymbol{x}) = \frac{1}{\text{erf}\left(\sqrt{6}\right)^3}\left(\frac{6}{\pi\Delta x^2}\right)^{\frac{3}{2}}\exp\left(-\frac{6|\boldsymbol{x}_p^{(m)} - \boldsymbol{x}|^2}{\Delta x^2}\right) \tag{5}$$

of characteristic length $\approx \Delta x$. This procedure is as much accurate as the local sample size is large ($\mathcal{N}_\mathcal{S}(\boldsymbol{x},t) \to \infty$). The local sample size may be defined as $\mathcal{N}_\mathcal{S}(\boldsymbol{x},t) = \tilde{n}_p(\boldsymbol{x},t)\Delta x^3$. The two-point correlation function computed from Eulerian fields is then defined as :

$$3R_\theta^{pp}(r) = \sum_{i=1}^{3} \overline{\frac{< \tilde{n}_p(\mathbf{x},t)\widetilde{T}_p(\mathbf{x},t)\tilde{n}_p(\mathbf{x}+r\mathbf{e}_i,t)\widetilde{T}_p(\mathbf{x}+r\mathbf{e}_i,t) >}{< \tilde{n}_p(\mathbf{x},t)\tilde{n}_p(\mathbf{x}+r\mathbf{e}_i,t) >}} \tag{6}$$

where $\mathbf{e}$ is the direction vector and angle brackets and over line denote instantaneous spatial average and temporal average, respectively. Under the assumption of homogeneous, isotropic, and statistically stationary flows, spatial and temporal averages represent the ensemble average over a large number of particle-laden flow realizations. Under such conditions, methods Eqn (1) and Eqn (6) are theoretically equivalent. Finally, the one-particle correlation, i.e. the particle temperature variance, is defined as

$$q_\theta^2 = \frac{1}{2}\overline{\left[T_p^{(m)}(t)T_p^{(m)}(t)\right]}, \tag{7}$$

where square brackets and over line denote instantaneous average over all the particles and temporal average, respectively. This quantity will be used to normalize all the computed two-particle correlation functions. According to the mesoscopic Eulerian formalism [20, 8, 15, 17] the particle temperature variance may be decomposed in a correlated and an uncorrelated contributions $q_\theta^2 = \tilde{q}_\theta^2 + \delta q_\theta^2$. The correlated contribution may be obtained from the particle Eulerian fields as follows:

$$\tilde{q}_\theta^2 = \overline{\frac{1}{2}\frac{< \tilde{n}_p(\boldsymbol{x},t)\widetilde{T}_p(\boldsymbol{x},t)\widetilde{T}_p(\boldsymbol{x},t) >}{< \tilde{n}_p(\boldsymbol{x},t) >}}. \tag{8}$$

This quantity may also be estimated by means of the two-point correlation functions. The amount of the correlated (respectively uncorrelated) contribution as a function of the particle inertia makes the object of the present investigation.

3. Numerical simulations

Simulations correspond to the dispersion of a particle cloud into a non-isothermal homogeneous, isotropic, statistically stationary turbulence in a fully periodic cubic box. Parameter of the turbulent field are given in Table 1. The regime is very dilute which implies that the inter-particle collisions and the turbulence modulation by the presence of the particles may be neglected. Computational domain is a cubic box of 128^3 cells, periodical in boundary conditions and of size $L_{box} = 0.128$ m. Twenty-four simulations with 40 millions particles are carried out in order to obtain local and instantaneous Eulerian fields, with sufficient high resolution at small scales, for various dynamic and thermal particle inertia. The sample size approximates the statistical population of particles over all the particle realizations $\mathcal{H}_p$ for a given fluid flow realization $\mathcal{H}_f$. The mean sample size at each time is $< \mathcal{N}_\mathcal{S}(\boldsymbol{x},t) > \approx 19$ which corresponds to the number of particle par cell at the initialization. Direct numerical simulations are performed in Fourier space using a pseudo-spectral code (NS3D) in which incompressible Navier-Stokes equations and an additional scalar equation are solved. Statistically stationary motion is ensured by accounting for a stochastic forcing in momentum equation written in wavenumber space [5]

$$\frac{\partial\hat{u}_{f,i}}{\partial t} + \left[\frac{\delta_{ij} - k_i k_j}{k^2}\right]\hat{N}_j = -\nu k^2\hat{u}_{f,i} + \hat{f}_i. \tag{9}$$

where $\hat{N}_j$ are nonlinear terms. The stochastic force is computed using a Langevin equation with a first order numerical scheme

$$\hat{f}_i^{n+1} = \hat{f}_i^n\left(1 - \frac{\Delta t}{T_F}\right) + \xi\sqrt{\frac{2\sigma_F^2\Delta t}{T_F}} \tag{10}$$

over the wavenumbers $[2k_0 - 6k_0]$, where $k_0 = 2\pi/L_{box}$, using a forcing time $T_F = 0.16$ s and a forcing amplitude $\sigma_F = 0.014$ m/s^2. According to Février et al. [8] such a wavenumber range represents a good compromise between the statistic contamination due to artifacts of the forcing scheme and the boundary conditions. In order to maintain the scalar field, a mean-scalar-gradient (along the y direction) forcing term is accounted for in the scalar fluctuation equation written in wavenumber space:

$$\frac{\partial\hat{\theta}_f}{\partial t} + \hat{N}(T) = -\alpha k^2\hat{\theta}_f - \hat{u}_{f,y}\zeta, \tag{11}$$

where $\hat{N}(T)$ are the scalar-velocity nonlinear terms, α is the thermal diffusivity and ζ a constant parameter set of the value

Table 1: Parameters of the turbulent flows

Dynamic quantities				Thermal quantities	
Reynolds number	Re_L	79	Prandtl number	Pr	0.7
Kolmogorov length scale	η_k/L_{box}	0.0046	Obukhov-Corrsin length scale	η_θ/L_{box}	0.006
Integral length scale	L_f/L_{box}	0.054	Thermal integral length scale	L_θ/L_{box}	0.067
Lagrangian time scale	T^L/τ_k	5.4	Thermal Lagrangian time scale	T^L_θ/τ_k	15.2

of 10 scalar units by meter. At each time step, fluid velocity and scalar fields are one-way coupled with a point-particle Lagrangian tracking method. The dilute mixture is composed by small ($d_p < \eta_k$) and heavy ($\rho_p >> \rho_f$) particles with an infinite solid thermal conductivity. When the gravity and radiative effects are neglected, the well-known equations governing the motion and heat exchange of each spherical, rigid and not rotating m-particle are:

$$\begin{aligned} \frac{\mathrm{d}\mathbf{x}_p^{(m)}}{\mathrm{d}t} &= \boldsymbol{v}_p^{(m)}, \quad \frac{\mathrm{d}\boldsymbol{v}_p^{(m)}}{\mathrm{d}t} = -\frac{1}{\tau_p}\left(\boldsymbol{v}_p^{(m)} - \mathbf{u}_{f@p}^{(m)}\right), \\ \frac{\mathrm{d}T_p^{(m)}}{\mathrm{d}t} &= -\frac{1}{\tau_\theta}\left(T_p^{(m)} - T_{f@p}^{(m)}\right) \end{aligned} \tag{12}$$

where $\mathbf{u}_{f@p}^{(m)}$ and $T_{f@p}^{(m)}$ are the undisturbed fluid velocity and temperature at the particle center location. For small heavy particles, the dynamic τ_p and the thermal τ_θ response times may be defined in the Stokes regime as

$$\tau_p = \frac{\rho_p d_p^2}{18\mu_f}, \qquad \tau_\theta = \frac{Pr\,\rho_p d_p^2 C_{pp}}{6Nu\,\mu_f\,C_{pf}} \simeq \frac{3}{2}\,Pr\,\beta\,\tau_p \tag{13}$$

where Pr is the Prandtl number chosen smaller than unity to ensure well-resolved thermal small scales, Nu the Nusselt number which reduces to 2 in the Stokes regime, μ_f the dynamic viscosity of fluid, ρ_p and d_p the particle density and diameter respectively and $\beta = C_{pp}/C_{pf}$ is the particle-to-fluid heat capacity ratio. Both fluid (nonlinear terms) and particles are time integrated by using an Adams-Bashforth second order scheme. Eulerian quantities at the particle location are obtained by a third-order Lagrange polynomial algorithm. Particles were randomly embedded in the statistically stationary turbulent flow, at the same velocity and temperature as the fluid. Before to start with post-processing particle data for statistics, simulations were made run for a time much greater than the particle response times in order to ensure convergence in particle moments (kinetic energy and temperature variance) and in preferential concentration as well. Twenty-four simulations were carried out for various particle inertia. They may be identified by three different classes following the ratio between the dynamic and the thermal particle response times: $\tau_p/\tau_\theta \sim 1$, $\tau_p/\tau_\theta > 1$, and $\tau_p/\tau_\theta < 1$, referred to as $A0$, $A1$ and $A2$ respectively. A summary of all the simulations is given in Table 2. An estimate of the ratio between Stokes numbers is also offered. The thermal (dynamic respectively) Stokes number St_θ (St) is defined as the ratio between the thermal (dynamic) response time τ_θ (τ_p) and the fluid integral thermal (dynamic) time scale sampled along particle trajectories $T^L_{f@\theta}$ ($T^L_{f@p}$). Dynamic and thermal Stokes numbers are here estimated using the well known Tchen's relation and the corresponding relation for the particle temperature variance as proposed by Derevich [4] and Zaichik et al. [25]:

$$q_p^2 = \frac{1}{1+St}q_{f@p}^2, \qquad q_\theta^2 = \frac{1}{1+St_\theta}q_{\theta@p}^2 \tag{14}$$

where $q_{f@p}^2$ and $q_{\theta@p}^2$ are kinetic energy and temperature variance of the fluid along the particle paths. It is however well known that these relations are not accurate when the Stokes numbers tend to zero since the autocorrelation functions no longer get an exponential behavior [25]. This mainly affect the estimate of the lower Stokes numbers in our simulations (the first two/three points in the Table 2).

Table 2: Ratio between response times and Stokes numbers (as estimated from Eq. (14)) and correlation coefficients.

ID	τ_p/τ_θ	St/St_θ	ξ_p	ξ_θ
A0	0.96	3.01	0.99	0.99
	0.96	1.22	0.96	0.96
	0.96	0.96	0.92	0.92
	0.96	0.89	0.86	0.84
	0.96	0.91	0.80	0.79
	0.96	0.96	0.74	0.73
	0.96	1.01	0.67	0.67
	0.96	1.13	0.52	0.53
	0.96	1.17	0.43	0.45
	0.96	1.20	0.32	0.34
	0.96	1.07	0.37	0.40
A1	2.04	2.07	0.67	0.81
	3.41	3.73	0.67	0.88
	5.46	6.66	0.67	0.93
A2	0.45	0.39	0.82	0.68
	0.27	0.22	0.89	0.70
	0.17	0.13	0.94	0.74
	0.24	0.19	0.89	0.68
	0.12	0.09	0.94	0.68
	0.36	0.37	0.54	0.39
	0.25	0.24	0.61	0.38
	0.44	0.41	0.67	0.53
	0.32	0.28	0.74	0.53
	0.22	0.19	0.80	0.53

4. Results and discussion

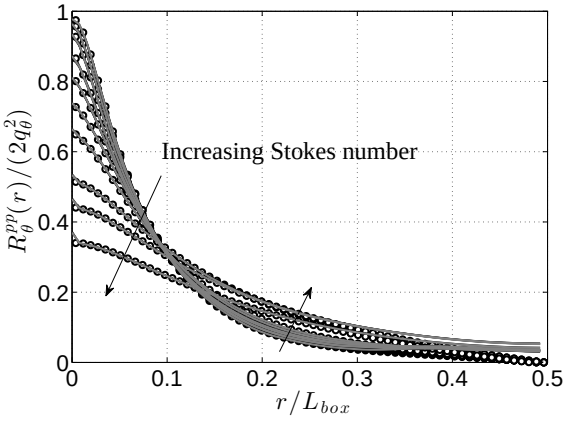

Figure 1: Two-point temperature correlation functions from $A0$.

The three methods presented in section 3 are here used to compute two-point correlation functions. Results from simulations $A0$ are depicted in Fig. 1. A zoom of the head of the functions is also given in Fig. 2. Very similar results have been found

when compared the three methods over low and intermediate distances, with the exception of higher Stokes numbers (first curves on the Fig. 2 from the bottom). Such higher Stokes numbers do not experience the phenomenon of preferential concentration, thus the local sample size will always stays around its mean value (~ 19), which makes statistics less accurate.

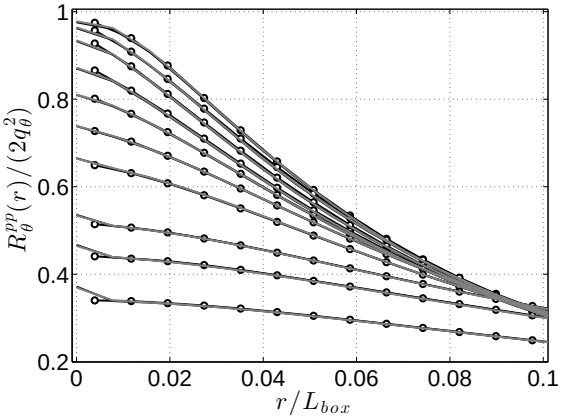

Figure 2: Zoom of Figure 1 for $r \to 0$.

For higher separation distances, methods Eqns (6)-(4) and Eqns (6)-(5) deviate from the classical lagrangian technique, Eqn (1). However, statistics are not conceptually the same since the methods Eqns (6)-(4) and Eqns (6)-(5) do not account for all the solid angles into the shell of radius r and, since the temperature field (as produced by a mean temperature gradient) is homogeneous but not isotropic, results should not be equivalent. Comparing the three methods on the correlation function $R^{pp}(r) = R_L^{pp}(r) + 2R_T^{pp}(r)$ where $R_L^{pp}(r)$ and $R_T^{pp}(r)$ are longitudinal and transversal functions of the particle velocity field, large distances are instead similar predicted (Fig. 3). Some differences between methods have been found at short distances when comparing longitudinal and transversal functions separately (not shown).

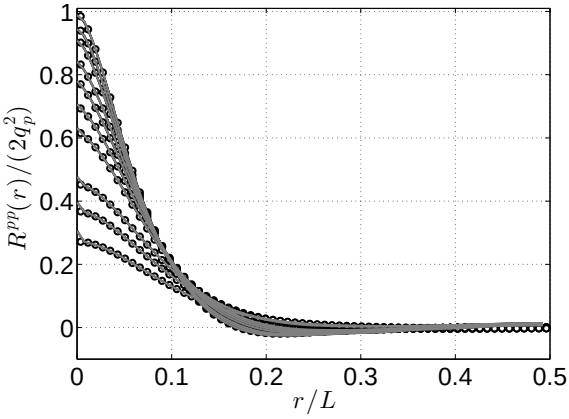

Figure 3: Two-point velocity correlation functions from $A0$.

Globally, the three methods exhibit similar predictions at short distances and can be alternatively used for assessing correlated and uncorrelated particle-properties contributions for $r \to 0$. The advantage of the methods Eqns (6)-(4) and Eqns (6)-(5) is that they are much less expensive in term of computational costs and they give an estimate at $r = 0$. In the following, method Eqns (6)-(5) will be retained for assessing the correlated and uncorrelated contributions at $r = 0$. Looking at the results depicted in Fig. 1, as expected, an increase in particle inertia points out the existence of a part of the temperature distribution that is not spatially correlated. This is consistent with the results of Février et al. [8] about the particle velocity distribution.

Velocity correlations of neighboring particles play an important role in the statistical modeling of the particle-particle interactions. In the frame of a presumed two-particle PDF approach, it has been shown [13, 21] that the amount of the correlated and the uncorrelated contributions may be written as follows:

$$\frac{\tilde{q}_p^2}{q_p^2} = \xi_p^2, \qquad \frac{\delta q_p^2}{q_p^2} = 1 - \xi_p^2 \tag{15}$$

where

$$\xi_p^2 = \frac{q_{fp}^2}{4 q_{f@p}^2 q_p^2}; \tag{16}$$

ξ_p is the fluid-particle velocity correlation coefficient which, according to the Cauchy-Schwarz inequality, is a function $\in [0, 1]$ and q_{fp} is the fluid-particle covariance. Using mesoscopic quantities, an equivalent correlation coefficient $\tilde{\xi}_p$ may be written as follows:

$$\tilde{\xi}_p^2 = \frac{\tilde{q}_{fp}^2}{4 \tilde{q}_{f@p}^2 \tilde{q}_p^2} \tag{17}$$

which is also constrained between zero and unity, $0 \leq \tilde{\xi}_p \leq 1$. Following the mesoscopic formalism, since the uncorrelated contribution of the particle velocity is not correlated with the undisturbed fluid velocity at the particle center location, by definition $\tilde{q}_{fp}^2 = q_{fp}^2$ and $\tilde{q}_{f@p}^2 = q_{f@p}^2$ [8]. This makes it possible to relate Eqn (17) with Eqn (16) and to deduce the following inequalities

$$\xi_p^2 \leq \frac{\tilde{q}_p^2}{q_p^2} \leq 1, \qquad 0 \leq \frac{\delta q_p^2}{q_p^2} \leq (1 - \xi_p^2) \tag{18}$$

which show that ξ_p^2 (respectively $1 - \xi_p^2$) derived by a two-particle PDF approach, represents in fact the minimum value (maximum value) than the correlated (uncorrelated) contribution can take under realizability conditions. Février et al. [8] and Simonin et al. [21] in homogeneous isotropic turbulence, and Vance et al. [22] in channel flows, pointed out a linear dependency of the correlated amount with the correlation coefficient ξ_p, i.e.:

$$\frac{\tilde{q}_p^2}{q_p^2} = \xi_p, \qquad \frac{\delta q_p^2}{q_p^2} = 1 - \xi_p. \tag{19}$$

In our simulations, the predictive ability of the model Eqns (19) is assessed and results depicted in Fig. 4. For a comparison purpose, the inferior (superior) limit, corresponding to Eqns (15), is also displayed. Results confirm the linear dependency already observed in the aforementioned literature. This dependency represents an empirical relation for which no analytical demonstration exists [21]. In the same spirit, an equivalent fluid-particle temperature correlation coefficient ξ_θ may be defined as follows:

$$\xi_\theta^2 = \frac{q_{f\theta}^2}{4 q_{\theta@p}^2 q_\theta^2}, \tag{20}$$

where ξ_θ is a function $\in [0, 1]$ and $q_{f\theta}$ is the fluid-particle temperature correlation. On the basis of the same theoretical development applied to mesoscopic thermal fields, the correlated and uncorrelated temperature amount may be written as

$$\frac{\tilde{q}_\theta^2}{q_\theta^2} = \xi_\theta^2, \qquad \frac{\delta q_\theta^2}{q_\theta^2} = 1 - \xi_\theta^2 \tag{21}$$

which, by construction, leads to the following inequalities:

$$\xi_\theta^2 \leq \frac{\tilde{q}_\theta^2}{q_\theta^2} \leq 1, \qquad 0 \leq \frac{\delta q_\theta^2}{q_\theta^2} \leq (1-\xi_\theta^2) \tag{22}$$

in which, ξ_θ^2 and $1-\xi_\theta^2$ denote inferior and superior limits for the correlated and uncorrelated contributions, respectively. Eqn (21) and the linear dependency

$$\frac{\tilde{q}_\theta^2}{q_\theta^2} = \xi_\theta, \qquad \frac{\delta q_\theta^2}{q_\theta^2} = 1-\xi_\theta \tag{23}$$

are also assessed in our simulations and results depicted in Fig. 5.

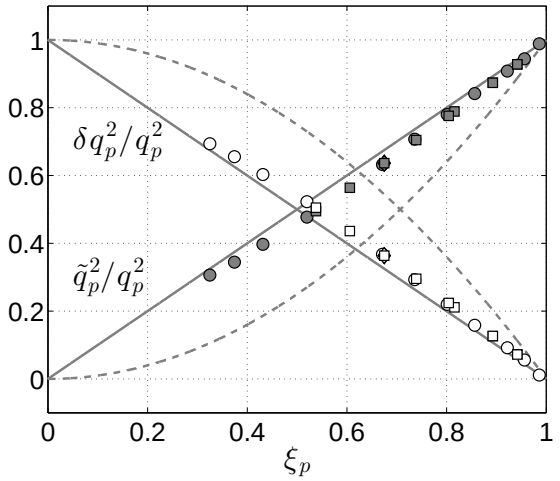

Figure 4: Amount of correlated and uncorrelated particle kinetic energy, $R^{pp}(0)/2q_p^2$. Circles: sim. $A0$, diamonds: sim. $A1$, squares: sim. $A2$. Solid line: ξ_p $(1-\xi_p$, respectively), dashed line: ξ_p^2 $(1-\xi_p^2$, respectively)

Contrary to what found for particle kinetic energy, the correlated and uncorrelated amount of the particle temperature variance do not match the predictions given by ξ_θ indiscriminately. The three classes behave in fact in a different way. In simulations $A1$, for which the thermal Stokes number is smaller than the dynamic Stokes number (diamonds in Fig. 5) results and predictions match very well, which means that the particle-particle thermal correlations only rely on the interactions between particle and fluid thermal scales as predicted by the correlation coefficient ξ_θ. Similar results are found for simulations $A0$ in which Stokes numbers are very close. Deviation from the model is instead found for simulations $A2$ for which an increase of the correlated contribution is observed with respect to the expectations. This feature illustrates that the thermal correlation between two particles may increase when the correlation in motion increase.

Correlations between neighboring particles depend on the their residence time in the same turbulent eddy compared to their response time [20]. Such a residence time relies on the relative velocity at which particles cross the turbulent eddy which, obviously, depends on their kinetic energy. It is therefore conjectured that particle-particle thermal correlations should also depend on the dynamic response time which defines their motion in a turbulent flows. The dependency of the particle-particle thermal correlations on both the dynamic and thermal Stokes numbers is under investigation.

Unfortunately, the mean-temperature gradient we used to force the scalar presents two main issues: i) the fluid temperature field is homogeneous but not isotropic, ii) the forcing introduces an additional low-frequency time scale (as it may be observed by Fig. 6). These concerns affect the physics of the particle-laden flows and make the analysis much more complex. Therefore, in order to proceed with the investigation, an alternative scalar forcing, inspired from the linear forcing proposed by Carroll et al. [2] is being used.

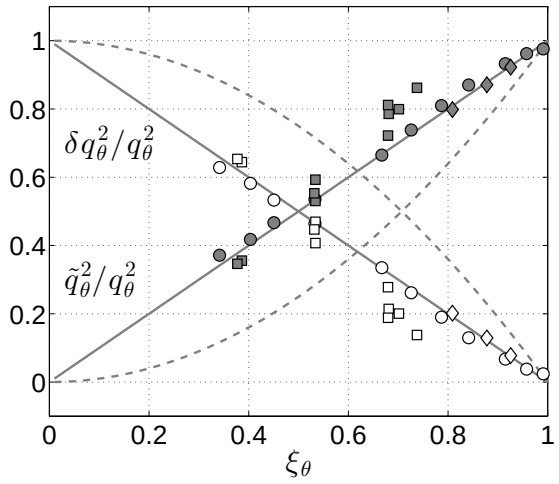

Figure 5: Amount of correlated and uncorrelated particle temperature variances, $R_\theta^{pp}(0)/2q_\theta^2$. Circles: sim. $A0$, diamonds: sim. $A1$, squares: sim. $A2$. Solid line: ξ_θ $(1-\xi_\theta$, respectively), dashed line: ξ_θ^2 $(1-\xi_\theta^2$, respectively)

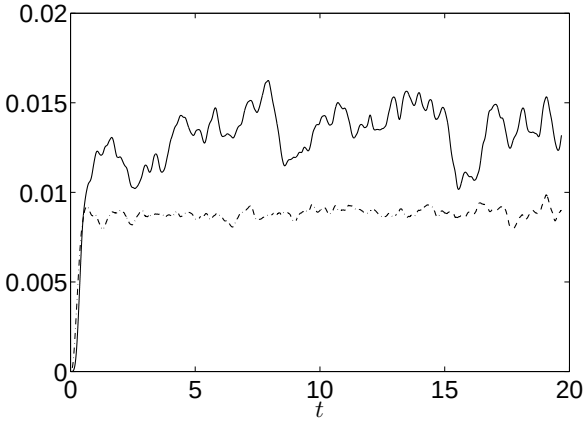

Figure 6: Kinetic energy (dashed line) and temperature variance (continuos line) of the turbulent fluid.

5. Aknowledgement

This work was granted access to the HPC resources of CALMIP supercomputing center under the allocation 2015-1208 and 2016-0111. CALMIP is gratefully acknowledged.

References

[1] Abrahamson, J., Collision rates of small particles in a vigorously turbulent fluid, *Chem. Eng. Sci.*, 30, pp. 1371–1379, 1975.

[2] Carroll, P.L., Verma, S. and Blanquart G., A novel forcing technique to simulate turbulent mixing in a decaying scalar field, *Phys. Fluids*, 25 (9), 095102, 2013.

[3] Chalons, C. , Massot, M. and Vié A., On the Eulerian Large Eddy Simulation of disperse phase flows: and asymptotic preserving scheme for small Stokes number flows, *SIAM Multiscale Modeling and Simulation*, 13 (1), pp. 291-315, 2015.

[4] Derevich, I. V., Velocity and temperature fluctuations in a turbulent suspension, *J. Eng. Phys*, 55 (1), pp. 716-722, 1988.

[5] Eswaran, V. and Pope, S.B., An examination of forcing in direct numerical simulations of turbulence, *Computer & Fluids*, 16 (3), pp. 257-278, 1988.

[6] Ferry, J. and Balachandar, S., A fast Eulerian method for dispersed two-phase flow, *Int. J. Multiphase Flow*, 27, pp. 1199-1226, 2001.

[7] Ferry, J. and Balachandar, S. Equilibrium Eulerian approach for predicting the thermal field of a dispersion of small particles, *Int. J. Heat Mass Transf.*, 48 (3-4), pp. 681-689, 2005.

[8] Février, P., Simonin O. and Squires, K. D., Partitioning of particle velocities in gas-solid turbulent flows into a continuous field and a spatially uncorrelated random distribution: theoretical formalism and numerical study, *J. Fluid Mech.*, 533, pp. 1-46, 2005.

[9] Fox, R.O., A quadrature-based third-order moment method for dilute gas-particle flows, *J. Comput. Phys.*, 227 (12), pp. 6313-6350, 2008.

[10] Hinze, J. O., *Turbulence*, McGraw-Hill, 1975.

[11] Kaufmann, A., Moreau, M., Simonin, O. and Helie, J., Comparison between Lagrangian and Mesoscopic Eulerian Modeling Approaches for Inertial Particles Suspended in Decaying Isotropic Turbulence, *J. Comp. Physics*, 227 (13), pp. 6448-6472, 2008.

[12] Laurent, F. and Massot, M., Multi-fluid modeling of laminar poly-dispersed spray flames: origin, assumptions and comparison of sectional and sampling methods, *Combust. Theor. Model.*, 5, pp. 537-572, 2001.

[13] Laviéville, J., Deutsch, E. and Simonin, O., Large Eddy simulation of interactions between colliding particles and a homogeneous isotropic turbulence field, *Gas-Solid flows*, ASME Vol. 228, pp. 347-358, 1995.

[14] Masi, E., Bédat, B., Moreau M. and Simonin, O., Euler-Euler large-eddy simulation approach for non isothermal particle-laden turbulent jet, *Proceedings of the ASME - Fluids Engineering Division Summer Meeting*, Jacksonville, Florida, USA, Vol. 1 , pp. 111-120, 2008.

[15] Masi, E., Simonin, O. and Bédat, B., The mesoscopic Eulerian approach for evaporating droplets interacting with turbulent flows, *Flow Turbulence Combustion*, 86, pp. 563-583, 2011.

[16] Masi E., Simonin O., Riber E., Sierra P. and Gicquel L.Y.M., Development of an algebraic-closure-based moment method for unsteady Eulerian simulations of particle-laden turbulent flows in very dilute regime, *Int. J. of Multiphase Flow*, 58, pp. 257-278, 2014.

[17] Masi, E. and Simonin O., Algebraic-Closure-Based Moment Method for Unsteady Eulerian Simulations of Non-Isothermal Particle-Laden Turbulent Flows at Moderate Stokes Numbers in Dilute Regime, *Flow Turbulence Combustion*, 92, pp. 121-145, 2014.

[18] Moreau, M., Simonin, O., and Bédat, B., Development of gas-particle Euler-Euler LES approach: a priori analysis of particle sub-grid models in homogeneous isotropic turbulence, *Flow, Turbulence and Combustion*, 84 (2), pp. 295-324, 2010.

[19] Riber, E., Moreau, V., Garcia, M., Poinsot, T. and Simonin, O., Evaluation of numerical strategies for large eddy simulation of particulate two-phase recirculating flows, *J. Comp. Physics*, 228, pp. 539-564, 2009.

[20] Simonin, O., Feṽrier, P. and Laviéville, J., On the spatial distribution of heavy particle velocities in turbulent flow: From continuous field to particulate chaos, *J. of Turbulence*, 3, 40, 2002.

[21] Simonin, O., Zaichik, L. I., Alipchenkov, V. M. and Février, P., Connection between two statistical approaches for the modelling of particle velocity and concentration distributions in turbulent flow: the mesoscopic Eulerian formalism and the two-point probability density function method, *Phys. Fluids*, 18, 125107, 2006.

[22] Vance, M. W., Squire K. D. and Simonin, O., Properties of the particle velocity field in gas-solid turbulent channel flow, *Phys. Fluids*, 18, 063302, 2006.

[23] Vié, A., Doisneau, F. and Massot M., On the Anisotropic Gaussian closure for the prediction of inertial-particle laden flows, *Communications in Computational Physics*, 17 (1), pp. 1-46, 2015.

[24] Yuan, C. and Fox, R.O., Conditional quadrature method of moments for kinetic equations, *J. Comput. Physics*, 230 (22), pp. 8216-8246, 2011.

[25] Zaichik, L. I., A statistical model of particle transport and heat transfer in turbulent shear flows, *Phys. Fluids*, 11, pp. 1521-1534, 1999.